Chemical Methodologies

Original Research Article

Determination of Fuconazole Using Flow Injection Analysis and Turbidity Measurement by a Homemade NAG-4SX3-3D Analyzer

Nagham Shakir Turkie, Sarah Faris Hameed*

Department of Chemistry, College of Science, University of Baghdad, Baghdad, Iraq

ARTICLE INFO

ABSTRACT

The research work exemplifies a sensitive, rapid, and simple procedure for measuring fluconazole using turbidity-continuous flow injection analysis for the generation of white precipitate via the reaction of fluconazole with phosphotungestic acid, and detecting the attenuation of incident light caused by light colliding with the precipitate surface grain using the NAG-4SX3-3D analyzer to determine turbidity (0-180˚). The linear range extended from 0.01-18 mmol.L^{-1} for fluconazole measurements were considerably lower than 0.5 RSD % for the repetition (n=6) for the concentration chosen (2, 13 mmol.L^{-1}), with limit of detection=7.5342 ng/sample from the gradual dilution over the lowest concentration on the calibration graph , linear dynamic range (r = 0.9989), (correlation coefficient), percentage linearity (R^2 percent = 99.79) traditional approaches (UV-spectrophotometric at λ_{max}=260 nm with linear range (0.001-1) mmol.L^{-1}, r=0.9987, R^2=0.9973, R^2%=99.73, and turbidimetric method with linear range (0.01-17) mmol.L^{-1} , r= 0.9869, R^2=0.9740, R^2%= 97.40 were compared with the suggested strategy. In comparison to the typical reference method's 10 mm irradiation, it was discovered, in addition to the technique's developed sensitivity and the use of minimal chemicals, that this approach is characterized by a dynamic system, which avoids precipitated particle setting during measurements. The results indicated that the developed method has a wide range of concentration with a high linearity and sensitivity. Furthermore, the continuous dilution in CFIA allows for the management of high or low concentrations, for a wider range of applications. The devised approach is believed to be the most acceptable for fluconazole molecule determination in pure and pharmaceutical formulations when compared with the reference methods. The method used in this research work is a pioneered developed approach and proved its success in determination of fluconazole in pure and pharmaceutical formulations.

GRAPHICAL ABSTRACT

Fluconazole   Phosphotungestic acid   Fluconazole-phosphotungestic acid
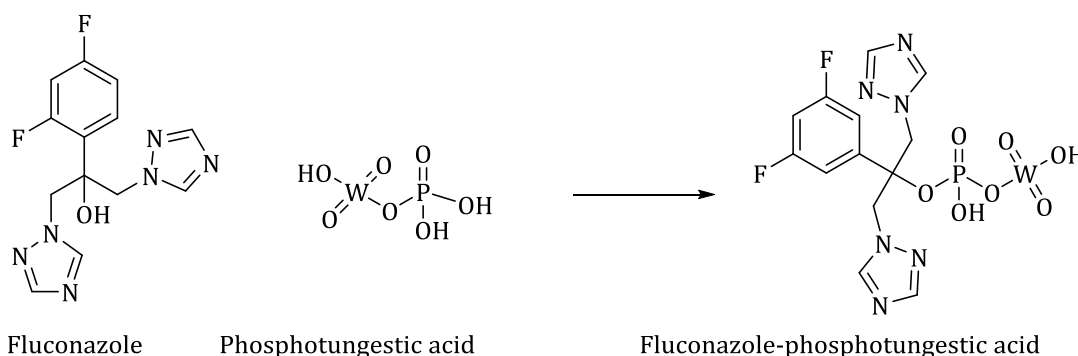
* Corresponding author: Sarah Faris Hameed
✉ E-mail: sarahf.hameed@yahoo.com

Introduction

Fluconazole (FLZ, 2-(2,4-difluorophenyl)-1,3-bis(1H-1,2,4triazole-1-yl)-propan-2-ol), as indicated in Scheme 1, that is commonly known as diflucanis [1], is an antifungal medication [2-4] prescribed by the United States Food and Drug Administration (FDA) to treat mucocutaneous candidiasis [5], such as esophageal candidiasis (infection of the esophagus), oropharyngeal candidiasis (infection of part of the throat), and vulvovaginal candidiasis (infection of the vulva and vagina), reduces candidiasis in people getting chemotherapy [6] and/or radiation after a bone marrow transplant. Meningitis caused by cryptococcal bacteria should be treated. Fluconazole is a fungistatic triazole drug that is used to treat systemic and superficial fungal infections. Fluconazole medication has been linked to temporary mild-to-moderate blood aminotransferase increases and clinically obvious acute drug-induced liver impairment. In 2004 and 2005, there were patent expirations. FLZ is a broad-spectrum tri azole antifungal agent that has emerged as a suitable substitute to amphotericin B in the treatment and prevention of various superficial and systemic fungal infections. It is a tri azole compound with potent antifungal activity that is currently being evaluated in clinical trials. The adverse effects [7-11] of fluconazole might range from skin lesions or skin rashes to pounding heartbeats, skin discomfort, breath shortness, dark urine, liver issues and changes in taste, stomach pain, major heart problems, abrupt disorientation, and others. A literature review reveals various techniques for determining fluconazole in biological fluids that have been documented such as UV spectrophotometric technique [12], and gas chromatography [13].

Materials and Methods

The solutions were produced using distilled water and all of the utilized chemicals were analytical reagent grade. By dissolving 1.2251 g of fluconazole in 100 mL of distilled water ($C_{13}H_{12}F_2N_6O$), a standard solution of 0.04 M fluconazole (molecular weight 306.271 g.mol^{-1}, BDH) was produced. 8.6406 g of phosphotungestic acid ($H_3PW_{12}O_{40}$,) having a molecular weight of 2880.2 g.mol^{-1} (Hopkin and Williams LTD) was dissolved in 250 mL of distilled water to make a standard solution.

Instruments

A flow cell was used which was produced from a homemade NAG-4SX3-3D analyzer. The output from the attenuation of incident light 0–180° was captured (Figure 1). The signal outputs were recorded using a potentiometric recorder (Siemens, Germany), Ismatic peristaltic pump with sample loop, and six-port injection valve (Teflon, variable length). The UV spectrophotometric (Shimadzu, Japan) and turbidimetry equipment were used for the traditional techniques. The proposed mechanism was depicted in Scheme 2.
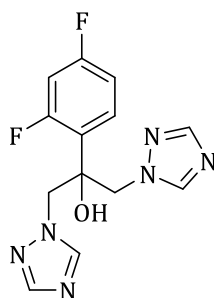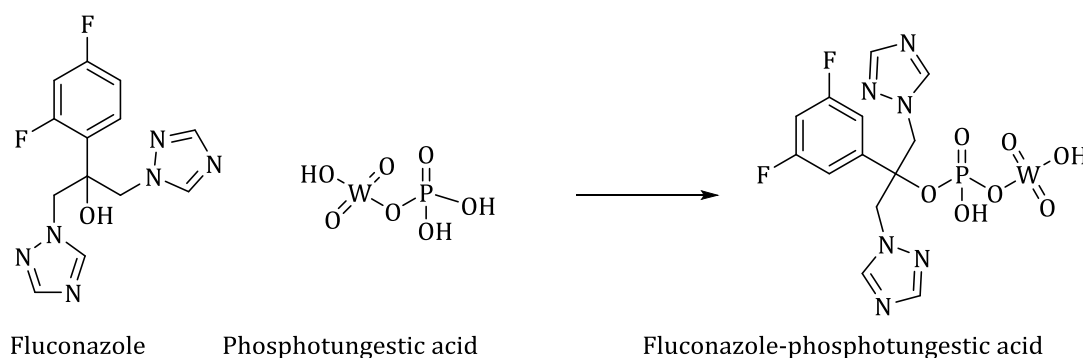

Fluconazole

Scheme 1: Fluconazole structure
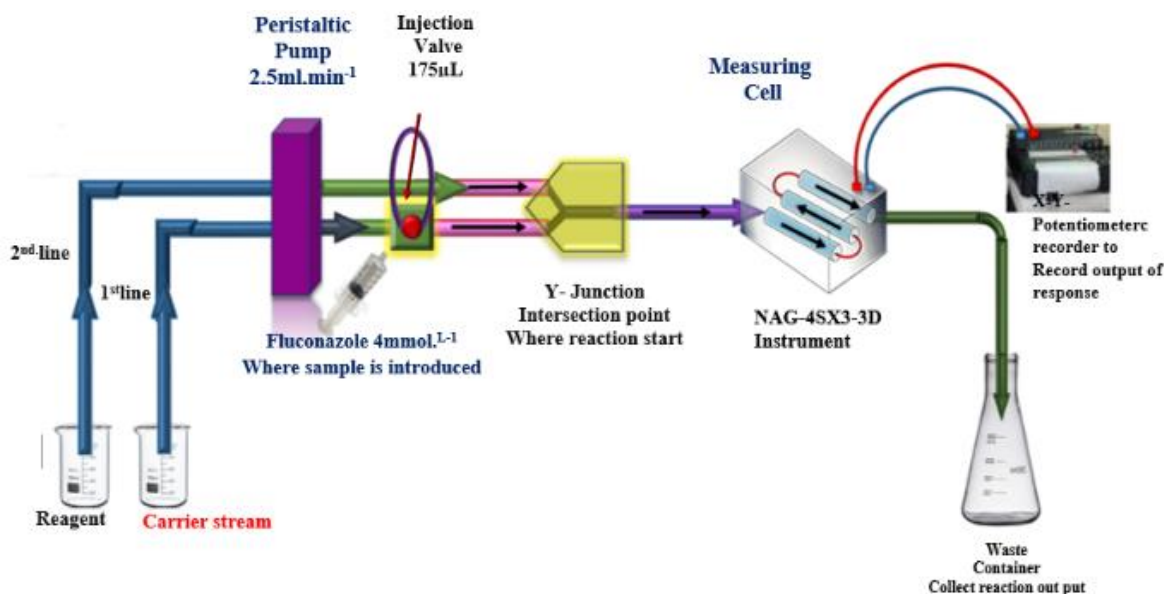
Figure 1: Diagram of system utilized to determine fluconazole via phosphotungestic acid

Fluconazole   Phosphotungestic acid   Fluconazole-phosphotungestic acid

**Scheme 2:** A possible mechanism for reaction of fluconazole with phosphotungestic acid

Influence of phosphotungestic acid concentration

To determine the optimal concentration, a series of phosphotungestic acid solutions ranging from (1-10) mmol.L^{-1} were produced. Fluconazole (5 mmol.L^{-1}) was utilized as a preliminary concentration in a 175 µL sample volume, and each measurement was performed three times. According to the results of the study, 7 mmol.L^{-1} of phosphotungestic acid was required to achieve the greatest attenuation of incoming light, as indicated in Table 1 and Figure 2. It can be revealed that an increase in phosphotungestic acid can cause an increase in particle due to the accumulating action of precipitate particles, density can reach up to 7 mmol.L^{-1}, after which there was a decrease in incident light attenuation corresponding to the same particle growth with increased phosphotungestic acid concentration.

Table 1: Effect of phosphotungestic acid on the measurement of energy transducer response S/N for determination of fluconazole

| [PTA] mmol.L^{-1}	Average $\bar{Y}Zi$ (mV) (n=3)	RSD%	95 percent confidence interval $\bar{Y}Zi$(mV)± t SEM
1	95	1.39	95±3.279
3	336	0.63	336±5.242
5	360	0.59	360±5.291
7	420	0.47	420±4.919
10	420	0.30	420±3.080
13	400	0.49	400±4.894
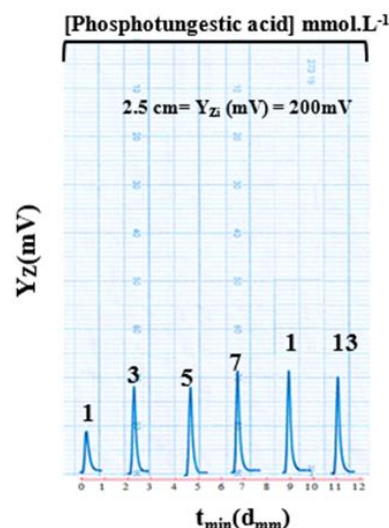
Figure 2: Various concentrations of phosphotungestic acid and its effect on (S/N) energy transducer response in mV

Influence of acid or salt media on fluconazole - phosphotungestic acid precipitation system

Using the optimal concentration of phosphotungestic acid solution 7 mmol.L^{-1}, the influence of acid and salt (50) mmol.L^{-1} in the reaction media on sensitivity, in general, was investigated. This investigation employed tartaric acid, sulfuric acid, acetic acid, hydrochloric acid, nitric acid, ascorbic acid, potassium chloride, ammonium acetate, ammonium chloride, sodium chloride, sodium nitrite, potassium iodide, sodium sulfate, and sodium carbonate, respectively. A preliminary physical condition was employed, with a volume of sample 175 µL with flow rate 2.5 mL.min^{-1}. Figure 3 depicts a distinct peak height of the measured response; leading to the conclusion that sulfuric acid can be utilized as optimum medium for the research work.
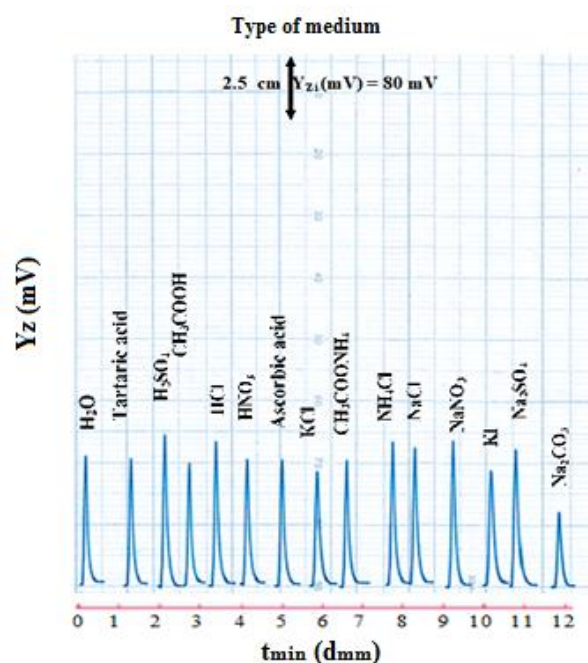
Figure 3: Effect of type of media on the profile using sample volume 175 µL, [Fluconazole]=4 mmol.L^1, [phosphotungestic acid]=7 mmol.L^{-1}, flow rate of carrier stream 2.5 mL.min^{-1} via the attenuation measurement of incident light expressed as a peak heights

Effect of sulfuric acid concentration

Using phosphotungestic acid 7 mmol.L^{-1}-fluconazole 4 mmol.L^{-1}- sulfuric acid system, the phosphotungestic acid system was constructed with a variable concentration of sulfuric acid ranging from (10-250) mmol.L^{-1} and a volume of sample 175 µL and a flow rate of 2.5 mL.min^{-1} for the carrier stream and reagent streams. Table 2 indicates a rise in peak height represented as an incident light attenuation with increasing sulfuric acid concentration, which might be connected to the creation of tiny solid particles that resulted in an increase in inter spatial distance and incoming light attenuation. Whereas up to 200 mmol.L^{-1} sulfuric acid concentration, as seen in Table 2, resulted in a reduction in S/N energy transducer response, which was likely related to precipitation particle dispersion. As a result, the optimal concentration of sulfuric acid was determined to be 200 mmol.L^{-1}.

Table 2: Effect of variable concentration of sulfuric acid on energy transducer response (S/N) of fluconazole (4 mmol.L^{-1}) - phosphotungestic acid system

| [H$_2$SO$_4$] mmol.L-1 (n=3)	average ȲZi(mV) (n=3)	RSD%	95 percent confidence interval ȲZi(mV)± t SEM
10	344	0.61	344±5.242
30	416	0.62	416±6.409
50	496	0.60	496±7.403
70	472	0.53	472±6.161
100	568	0.46	568±6.509
130	620	1.08	620±16.595
150	640	0.39	640±6.161
170	688	0.37	688±6.260
200	732	0.32	732±5.764
250	720	0.30	720±5.341

Physical variable

Influence of flow rate

To choose the optimum flow rate that varied from 1-4 mL.min^{-1} for carrier stream and phosphotungestic acid stream with 175 µL of sample volume, the optimal concentration of the reactant: phosphotungestic acid (7 mmol.L^{-1}), and the initial concentration of fluconazole (4 mmol.L^{-1}) were used. Figure 4 summarizes the results. As demonstrated in this figure, there was a rise in peak height with an increase in Δt$_b$ with an increase in flow rate, dispersion, and dilution resulted in a longer sample segment of the precipitate product, which was attributable to dispersion and dilution. While higher flow rates for the carrier stream and reagent resulted in a reduction in peak height, this could be due to the rapid departure of precipitate particles from the measuring cell, so the most efficient flow rate for fluconazole-phosphotungestic acid accomplishment was 2 mL.min^{-1} to obtain a regular response, sharp maxima, and reduce reactant solution consumption.

Influence the volume of sample on S/N transducer energy response in mV

Using a phosphotungestic acid (7 mmol.L^{-1})-fluconazole (4 mmol.L^{-1}) precipitation system with a 2 mL.min^{-1} flow rate. An open valve mode was used to inject a variable volume (82-281) µL of sample into the injection valve, allowing for removing samples from the sample loop on a continual basis. Figure 5 displays a plot of incoming light attenuation vs time. As demonstrated in this figure, increasing the sample volume up to 82 µL resulted in a considerable drop in response height and was more detectable than a high volume. This was owing to an increase in the width Δt$_B$ and response maxima, which may be ascribed to the continuous substantially, the section of precipitate particles in front of the detector has a greater temporal length, as well as an increase in particle size, leading precipitate particles to move slowly. Therefore, the optimal sample volume was determined to be 82 µl.
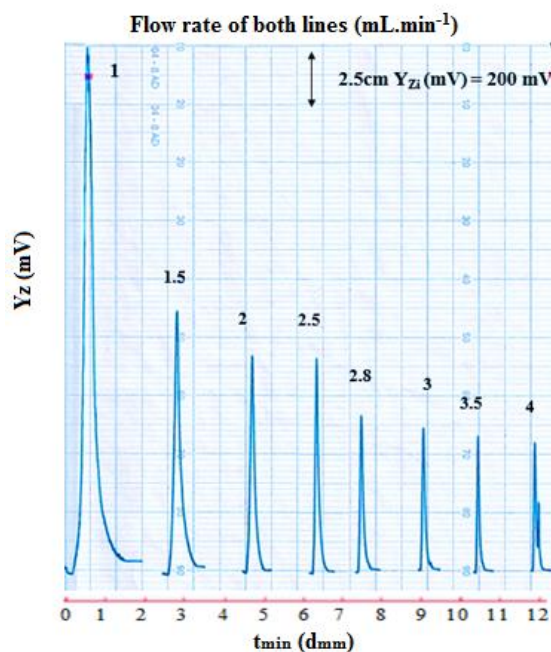
Figure 4: Profile at variable flow rate of versus $t_{min}(d)_{mm}$
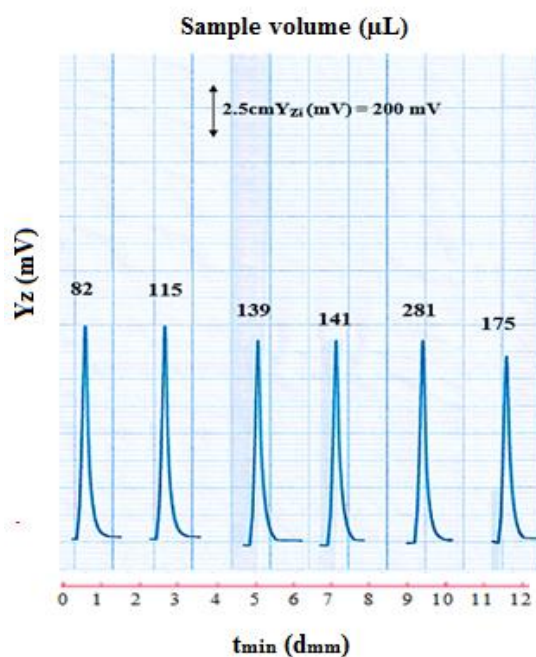
Figure 5: Effect of the different sample volume based on the response of an energy transducer via time using flow rate 2 ml .min^{-1} of reagent and carrier stream, fluconazole (4 mmol/L)- phosphotungestic acid (7 mmol/L) system

Effect of reaction coil length in μL

The influence of reaction coil length was investigated using a coil length ranging from 0 to 30 cm and an I.D of 1 mm. This length range has a volume of 0 to 942 μL, which was linked directly into the flow system following the Y-junction in Table 3. The fluconazole solution (4 mmol.L^{-1}) was employed as the optimal concentration for the precipitation system, with 175 μL as the injected sample volume. Table 3 clearly depcits that as coil length, Δt_B, and arrival time of injected sample from injection valve to measure flow cell increase, peak height decreases, which could be attributed to the increased effect of dilution and dispersion zones of sampling, as well as the continuous longer time duration of precipitate species in front of the detector.

Table 3: Effect of different reaction coil on the measurement of energy transducer response for determination of fluconazole

Coil Length segment cm r= 0.5	Coil length (µL)	Response output $\bar{Y}_{zi}$(mV) (n=3)	RSD%	95 percent confidence interval $\bar{Y}_{zi}$(mV)± t SEM	Δt_{sec}	Vadd (ml) at flow rate	C (mmo.L⁻¹)	D.F	t_{sec}
Without	0	784	0.14	24	1.682	0.195	20.5130	784±2.683	3
10	314	816	0.13	42	2.882	0.114	35.1463	816±2.733	18
20	628	792	0.15	48	3.282	0.100	40.0241	792±2.931	20
25	785	720	0.18	54	3.682	0.089	44.9024	720±3.279	21
30	942	672	0.18	57	3.882	0.084	47.3415	672±3.006	24

Effect of Y-junction on profile response

The Y-junction is needed in the process to mix the reactants. The Y-junction was added before the cell was measured directly the system of flow. The response pattern was examined when the Y-junction was changed in various parameters. For illustrating with a sample capacity of 175 µL and a flow rate of 2.5 mL.min⁻¹, fluconazole at its optimal concentration (4 mmol.L⁻¹) was utilized for both the carrier stream and the reagent. Figure 6 shows how the S/N transducer's energy response affects the Y-junction (meeting zone). Using varied volume mixing chambers and a larger diameter intersecting point, the effect on particle agglomeration, regulation, and regular distribution prior to the flow tube's entry was investigated. Particle scattering and dispersion, as well as increasing inter spatial distances; reduce the ability of incident light to raise the height of the energy transducer's response measurement, as indicated in Table 4. As a consequence, it was assumed that by employing a manifold unit with two 3 mm (inter diameter) entries and a 3 mm (inter diameter) output.
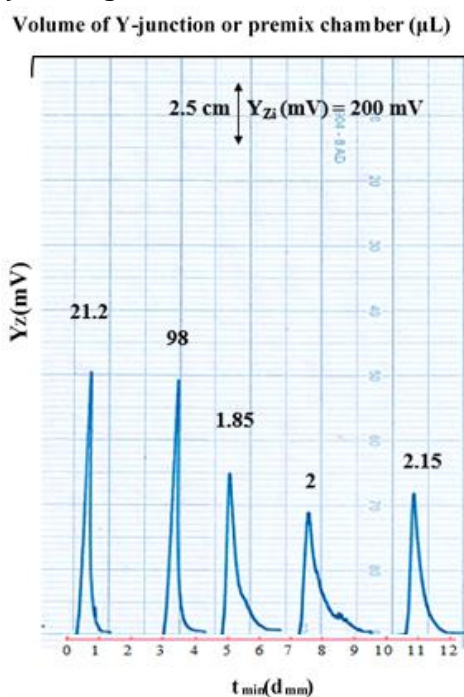
Figure 6: Effect of Y-junction on S/N energy transducer response versus $t_{min}(d)_{mm}$

Table 4: Effect of the variation of Y-junction on the attenuation of incident light by using 4 mmol.L^{-1} concentration of fluconazole and 7 mmol.L^{-1}, concentration of phosphotungestic acid, and flow rate of the carrier stream 2 mL.min

Kinds of Y-junction		Volume = $\pi r^2 h$	Output response average $\bar{Y}_{Zi}$(mV) (n=3)	t_{sec}	Volume mL	C (mm/L) DF
					At junction point	
Intersection junction point	3 mm (inter diameter) 3 mm, (thickness)	21.2μL	816	16	1.1699	0.2804 14.2667
	5 mm (inter diameter) 5 mm, (thickness)	98.00 μL	792	16.5	1.2800	0.2563 15.6098
Premix chamber	14 mm (inter diameter) 12 mm, (thickness)	1.85 ml	504	17	3.0653	0.1070 37.3821
	14mm (inter diameter) 13 mm, (thickness)	2.00 ml	384	18	3.2820	0.0999 40.0244
	14 mm (inter diameter) 14 mm, (thickness)	2.15 ml	440	18.5	3.4653	0.0947 42.2602

Estimating the linear dynamic range of fluconazole on a scatter plot of the S/N energy transducer response

Both physical and chemical variables were adjusted to their best possible values in the previous section (fluconazole–phosphotungestic acid (7 mmol.L^{-1})–H$_2$SO$_4$ (200 mmol.L^{-1}) system, 175 μL volume of sample, 82 μL reaction coil, and 2.0 mL.min^{-1} as a flow rate for carrier stream and phosphotungestic acid line (Figure 7**a**), and a set of series 0.01–25 mmol.L^{-1} solutions were prepared). The profile seen in Figure 7**b** is represented by a scatter-plot with a correlation coefficient of 0.9858 over the range of 0.01-18 mmol.L^{-1} (i.e. picking all twenty-seven points). Table 5 shows the analytical range that explains an increase in fluconazole concentration causes an increase in precipitate particulates (i.e. deals with directly proportional between fluconazole concentration and S/N energy transducer response) up to 18 mmol.L^{-1} (n = 23point) with r=0.9989 at the range of (0.01-18) mmol.L^{-1}. A broad maxima of the peak height was also observed above 18 mmol.L^{-1}, which could be attributed to an increase in precipitate particulates and their compactness, resulting in a reduction in interstitial spaces and reflecting surfaces, as well as an increase in particle size, resulting in a slower movement of particles, which resulted in a longer time duration of particles in front of the detector, resulting in a distorted response (Figure 7**b**).
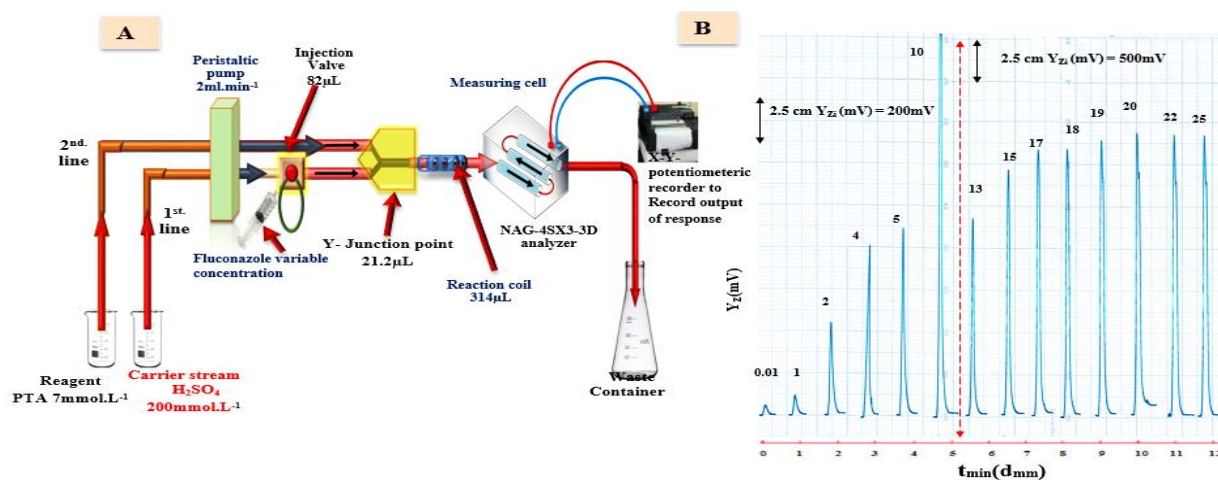
Figure 7: a) Design of system used for the determination of Fluconazole by phosphotungestic acid, b) Some of output response versus time, potentiometric scanning speed 1cm.min^{-1}

The working range was 0.01-19 mmol.L^{-1} (n = 24) with r = 0.9985, the scatter plot range was 0.01-25 mmol.L^{-1} (n = 27) with r = 0.9858, the dynamic analytical range was 0.01-22 mmol.L^{-1} (n = 26) with r = 0.9945 and the linear dynamic range was 0.01-18 mmol.L^{-1} (n = 23) with r = 0.9945. As a result, to improve the mathematical construction of the evaluation, a shorter range should be employed. The best-fit linear equation for the relationship between fluconazole concentration (independent variable) and diverging light (a parameter that is dependent) has r = 0.0.9989 and a percent capital R-squared of 99.97 percent (Table 5) on the following form:

$$\hat{Y}zi(mV) = 150.695 \pm 126.655 + 156.998 \pm 10.999 [\text{fluconazole}] \text{ mmol.L}^{-1}$$

Table 5: Different ranges for the Fluconazole concentration versus absorbance and scatter light using spectrophotometer and Turbidimetry method (classical methods) and NAG-4SX3-3D analyzer

Kinds of range	Range of [Flu] mmol.L^{-1}	$\hat{Y}_{Zi}$=a ± S$_a$t+b($\Delta y /\Delta x_{mmol/L}$) ± S$_b$ t [Flu] mmol.L^{-1} at confidence level 95%, n-2	R r^2 R^2%	t $_{tab}$ at 95%, n-2	Calculated t-value t$_{cal}$=/r/√n-2 / √1-r^2
		UV- Spectrophotometer at λ $_{max}$= 260nm			
		Developed NAG-4SX3-3D analyzer			
		Turbidity			
Linear range or linear dynamic range	0.001-1 (16)	0.083±0.026+1.694±0.052 [Flu] mmol.L^{-1}	0.9987 0.9973 99.73	2.145<< 7.124	
	0.01-18(23)	54.9825±32.4357+178.667±3.7620 [Flu] mmol.L^{-1}	0.9989 0.9979 99.79	2.079 << 3.525	
	0.01-17(19)	25.432±10.328+13.694±1.146 [Flu] mmol.L^{-1}	0.9869 0.9740 97.40	2.110 << 5.196	
Working range or calibration range	0.001-1.3 (17)	0.117±0.072+1.546±0.128 [Flu] mmol.L^{-1}	0.9888 0.9777 97.77	2.131 << 3.383	
	0.01-19 (24)	64.5067±39.9400+175.9900±4.2998 [Flu] mmol.L^{-1}	0.9985 0.9970 99.70	2.074 << 3.350	
	0.01-18(20)	26.495±10.665+13.354±1.103 [Flu] mmol.L^{-1}	0.9864 0.9729 97.29	2.101 << 5.219	
Dynamic range or analytical range	0.001-1.5 (18)	0.152±0.102+1.408±0.155 [Flu] mmol.L^{-1}	0.9794 0.9592 95.92	2.120 << 3.180	
	0.01-22(26)	102.1298±78.8468+166.8577±7.3962 [Flu]mmol.L^{-1}	0.9945 0.9891 98.91	2.064 << 2.673	
	0.01-19(21)	27.838±11.346+12.966±1.101 [Flu] mmol.L^{-1}	0.9847 0.9697 96.97	2.093 << 5.135	
Scatter plot	0.001-2 (20)	0.240±0.155+1.131±0.181 [Flu] mmol.L^{-1}	0.9518 0.9059 90.59	2.101 << 3.262	
	0.01-25(27)	150.6950± 126.6551+156.9984±10.9994 [Flu]mmol.L^{-1}	0.9858 0.9719 97.19	2.060 << 2.451	
	0.01-20(22)	29.681±12.706+12.481±1.162 [Flu] mmol.L^{-1}	0.9806 0.9617 96.17	2.086 << 4.873	

The scatter plot was able to explain a large portion of the n = 27 data. The new developed methodology for determining fluconazole was compared with the existing reference methods, namely the spectrophotometric method, as demonstrated in Figure 8**a** and the turbidity method in Figure 8b while Figure 8c represents the optimum concentration of phosphotungestic acid reacted with Fluconazole (4 mmol.L-1) in the presence of the best H_2SO_4 concentration of turbidimetric method, both of which are based on the absorbance measurements for a variable range of concentration, as indicated in Table 5 at λ_{max} 260 nm, and as depicted in Figure 9. The

optimal linear range of n = 23 is 0.01 to 18mmol.L⁻¹. It has a correlation coefficient of 0.9989 and a percent capital R-squared of 99.79 percent (Table 5).

Detection limit

The detection limit for fluconazole was estimated using three distinct strategies, theoretically, using the slope value; and practically, using progressive dilution for the lowest concentration from a scatter plot [14-16]. Using the precipitating agent phosphomolybdic acid, the fluconazole limit of detection was calculated, as indicated in Table 6.
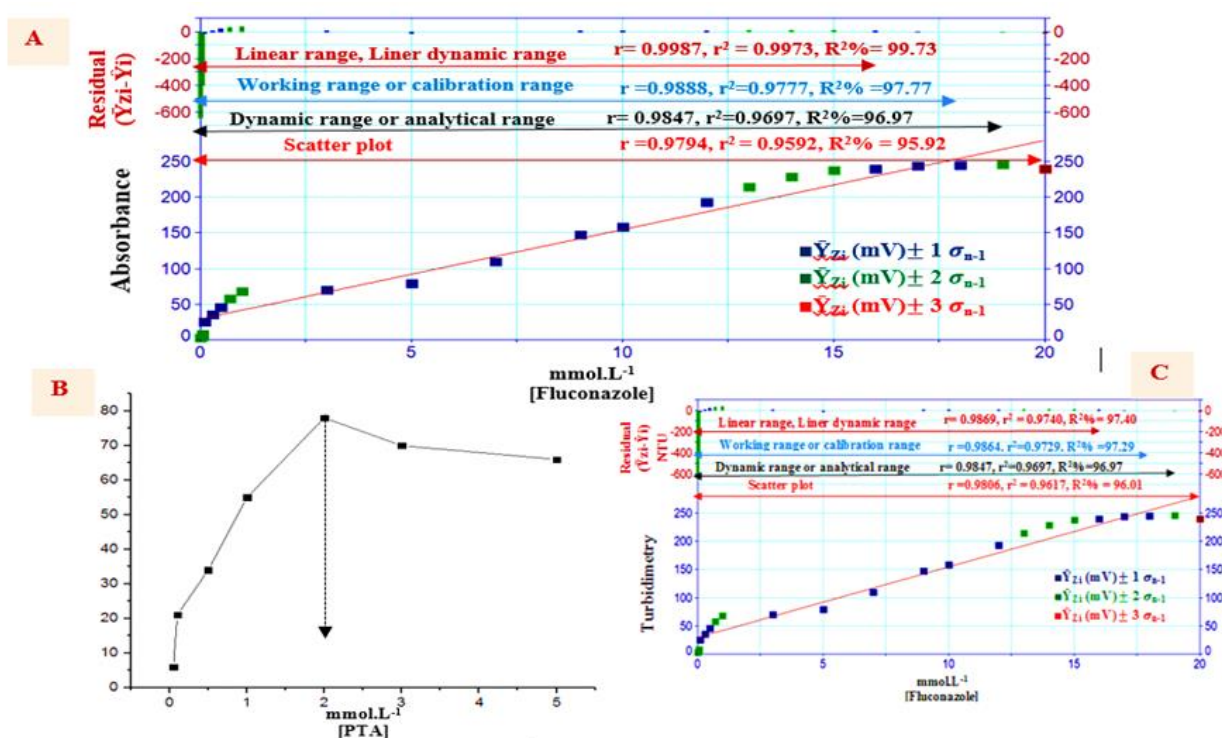
Figure 8: A: Various ranges for the impact of Fluconazole concentration on incident light attenuation using the NAG-4SX3-3D analyser, B: Graphical representation shows the optimum concentration of phosphotungestic acid reacted with Fluconazole (4 mmol.L⁻¹) in the presence of the best H_2SO_4 concentration of Turbidimetric method, C: The scatter plot for [Fluconazole] using turbidimetric method
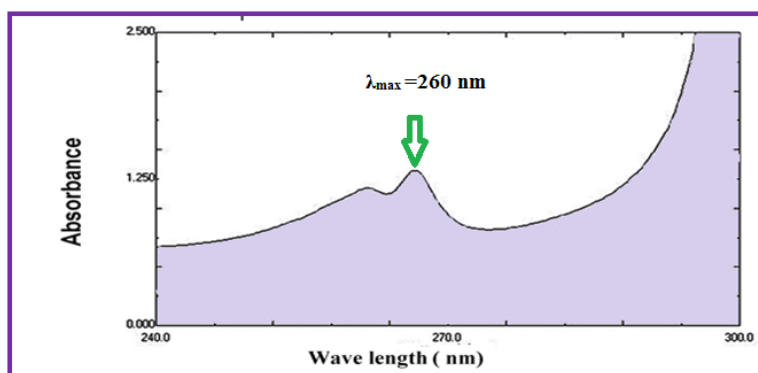
Figure 9: UV- spectrum for fluconazole at λ_{max} = 260 nm

Table 6: Detection limit of Fluconazole-phosphotungestic acid using 175 μL as an injection sample and best parameters using Fluconazole (4 mmol.L^{-1})-[phosphotungestic acid] (7 mmol.L^{-1})- H_2SO_4 (200 mmol.L^{-1}) system

Practically, the minimum concentration in a scatter plot is based on the continuous dilution.		Theoretical based on the slope value $x=3S_B/slope$	Theoretical based on the linear formula $\hat{Y} = Y_b + 3S_b$	Limit of quantitative L.O. Q $\hat{Y} = Y_b + 10S_b$
Developed approach (0.0003)mmo.L^{-1} for flu in PTA	Classical method			
	spectrophotometric method			
	(0.0003) mmol.L^{-1} for flu			
	Turbidmetric method (0.007) mmol.L^{-1} for flu in PTA system			
7.5342 ng/sample	15.3135 μg/sample	0.5233μg sample	21.5646 μg/sample	71.8820 μg/sample

Repeatability

The RSD given as a percentage in Table 7 is equivalent to the measurement's repeatability. A series of six injections were tested at a constant fluconazole concentration. Two different concentrations of fluconazole were used (2 and 13 mmol.L^{-1}) [17-19]. The relative standard deviation, as indicated in Figure 10, was less than 0.5%.

Table 7: Repeatability of fluconazole at the best parameters with 175μl sample volume

Concentration of molecule mmol.L^{-1}	$\bar{Y}_{Zi}$ (mV)output response average (n=6)	RSD%	Confidence interval at 95% $\bar{Y}_{zi}$ (mV)± t$_{0.05/2}\sigma_{n-1}/\sqrt{n}$
2	440	0.30	440±1.3087
13	2320	0.10	2320±2.328
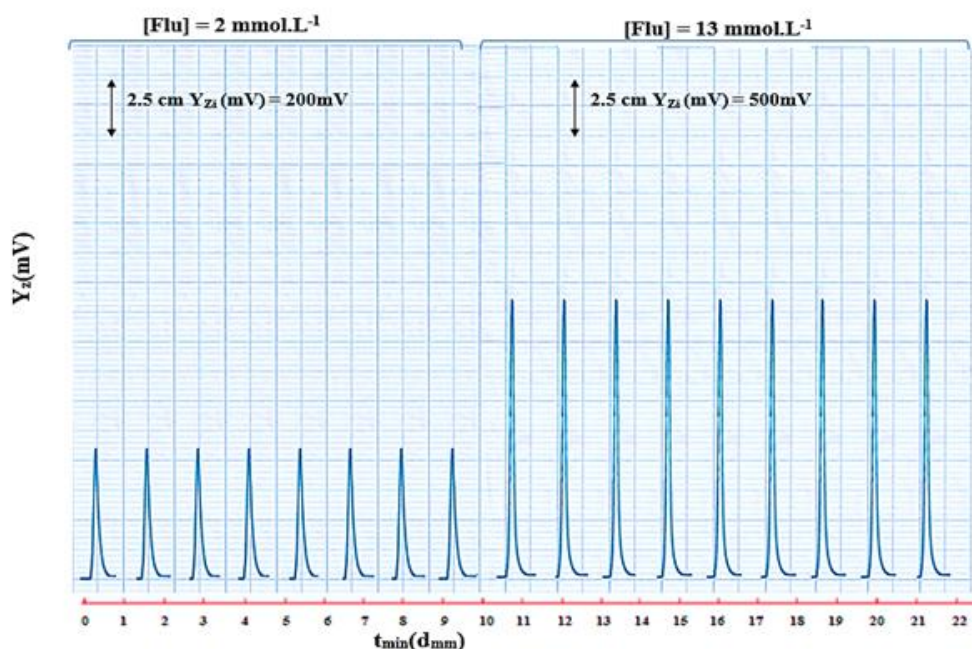
Figure 10: Repeatability of fluconazole peak height in mV at optimum parameters with 175μl sample volume

Estimation of fluconazole in drugs utilizing NAG-4SX3-3D analyzer

Fluconazole was determined in four samples of medicines from four different firms (Fluconazole, Vassil, Bulgaria, 150 mg), (Candeur, Tabuk, Saudi Arabia, 150 mg), (Fluconazole, Bristol, UK, 150 mg), (Fluconazole, Bristol, UK, 150 mg), and (diflucan, Pfizer, France, 150 mg) using the latest advanced technique (NAG-4SX3-SD analyzer). The

continuous flow injection analysis was combined with two methods: The UV-spectrophotometric measurement of absorbance at λ_{max}=260 nm and turbidimetric measurement of incident light attenuation at 0-180° for pale yellow fluconazole precipitate that reacted with phosphomolybdic acid using a homemade NAG-4SX3-3D analyzer. The data were mathematically addressed using the standard addition procedure, as displayed in Figure 11.
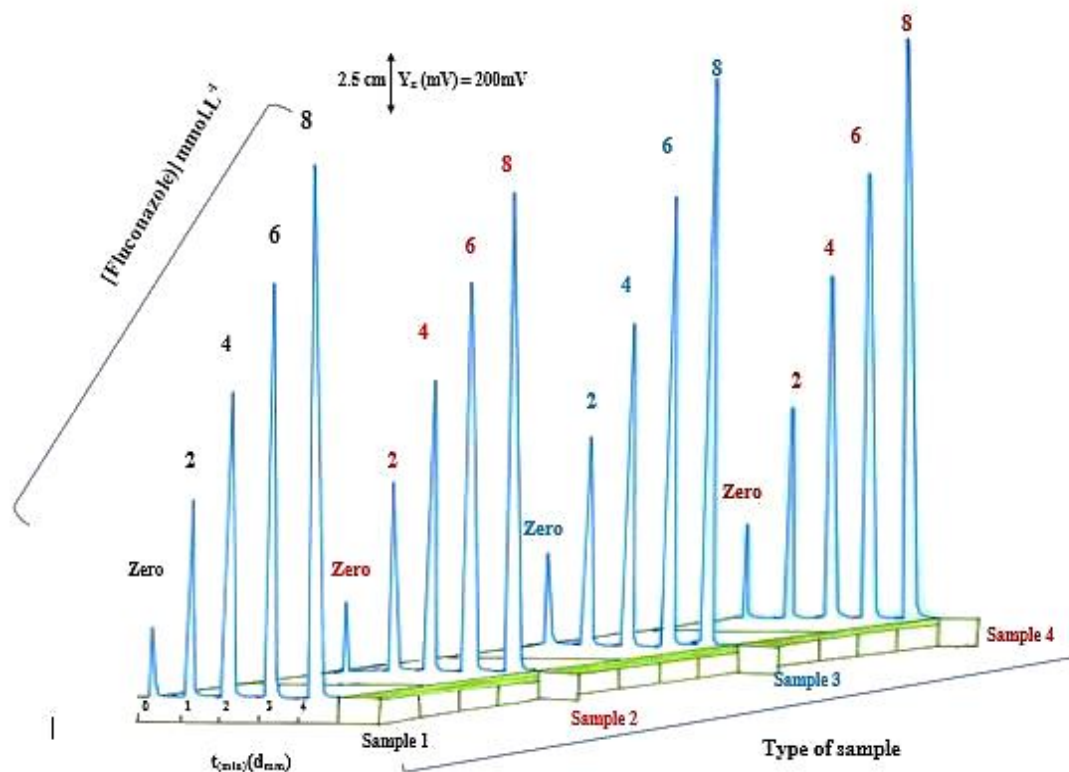
Figure 11: Peak height in mV for standard addition method for Fluconazole –phosphotungestic acid system using four different companies: Sample 1: Fluconazole, 150 mg, Vassil, Bulgaria; Sample 2: Candeur, 150mg, Tabuk, Saudi Arabia; Sample 3: Fluconazole, 150 mg, Brustol, UK; Sample 4: Dflucan, 150 mg, Pfizer, France

Table 8**a** shows the practical content of an active component at a 95% confidence level, as well as the (t-test) efficiency of determination (Figure 12), this depicts a comparison between two paths: 1- Comparison of the created technique NAG-4SX3-3D analyzer with the official stated value (150 mg) as Table 8**b** by calculating t-values for each individual corporation and comparing them to the tabulated t-value, the following is a formula for estimating a hypothesis: The null hypothesis is that there is no significant difference between the means derived from four distinct sources ($\overline{W_t}$) and the stated value (μ)

$$i.e;\ H_\circ: \overline{W_t} = \mu\ (150mg)$$

Alternative hypothesis: the means and quoted value are significantly different.

$$i.e;\ H_1: \overline{W_t} \neq \mu\ (150mg)$$

Because some obtained values exceeded t table (4.3030) at 95 percent confidence level and degree of freedom = 3, the null hypothesis was rejected and the alternative hypothesis was accepted, implying that there is a significant difference between the quoted active ingredient value and the measured value.

2- For the comparison of new methodology employing the NAG-4SX3-3D analyzer with two conventional methods UV-spectrophotometric method and turbidity, a paired t-test at α= 0.05 (2 tailed) was used. Table 8a indicates the measurement of incident light attenuation, taking into consideration that all medications from various multiple companies belong to the same

population, ignoring individual differences between manufacturers.

Assumption

Null hypothesis

$$H_\circ: \mu_{\text{NAG-4SX3-3D analyzer}} = \mu_{\text{UV- spectrophotometric}} = \mu_{\text{turbidity}}$$

There is no significant difference in the means of the two approaches.

Alternative hypothesis

$$H_1: \mu_{\text{NAG-4SX3-3D analyzer}} \neq \mu_{\text{UV- spectrophotometric}} \neq \mu_{\text{turbidity}}$$

The obtained data reveal that there was no significant difference between the devised approach, UV-spectrophotometric method, and turbidity method at 95 percent, α = 0.05 confidence interval, as shown in Figure 12 and Table 8**b**.

Statistical treatment of result by (one-way variance analysis)

The study employed a one-way ANOVA [20] (F-test) treatment, which compares three or more means, but only has one variable. The NAG4SX3-3D analyzer was evaluated for fluconazole measurement in various pharmaceuticals using a reaction of fluconazole with precipitating reagent phosphotungestic acid in the presence of H_2SO_4 and compared with three traditional methods (i.e., official method, Turbidity, and the UV-spectrophometric method), as depicted in Figure 13.

The F-test assumption for comparing three or more means. The first estimate is referred to as between – group variance (MS_B) or between – group variance (MS_B) (S_B^2). The second estimate, the within-group variance (MS_W) or (S_W^2), is computed using the data and is entirely unaffected by mean differences, but is dependent on variance

(i.e., S_i^2 = n-12). If there are no variations in the means, the estimated between-group variance will be almost equal to the within-group variance, resulting in an F-value of 1. The alternative hypothesis will be accepted and the null hypothesis will be rejected if the F-test value is larger than 0.5. This process is known as variance analysis (ANOVA) [21].

The ANOVA-test was used with a significance level of α = 0.05. (95 percent confidence level). Table 9 shows the results of an ANOVA test and a comparison of four Fluconazole samples.

The hypothesizes

(Null hypothesis) (H_0)

$$H_0 = \mu_{\text{fluconazole- Bulgaria}} = \mu_{\text{Candeur- Saudia Arabia}} = \mu_{\text{fluconazole- UK}} = \mu_{\text{Diflucan – Pfizer}}$$

In terms of the output of data, there is no significant variation between all used means of each sample from different companies. There is a considerable difference in all mean values, according to the option given.

H_1 (alternative hypothesis)

$$H_1: \mu_{\text{Fluconazole- Bulgaria}} \neq \mu_{\text{Candeur- Saudia Arabia}} \neq \mu_{\text{Fluconazole – UK}} \neq \mu_{\text{Diflucan- Pfizer}}$$

The collected information, presented in Table 9, reveals a substantial difference between the means of samples, with F_{Cal} (3.559801) more than F_{tab} (3.490295) for the Fluconazole-phosphotungestic acid system.

As a result, the null hypothesis will be rejected, and the alternative hypothesis will be accepted. This means that there are considerable variances in the samples utilized by four separate companies (four samples).

Table 8a: Standard addition data for the estimation of fluconazole in four samples of drugs using NAG-4SX3-3D analyser for fluconazole with phosphotungestic acid system and two classical methods

No. of sample	Commercial Name, Company Content Country	Confidence interval for the average weight of Tablet w̄i ± 1.96 $\sigma_{n-1}/\sqrt{n}$ at 95% (g)	Weight of Sample equivalent to 0.1531 gm (10 mmol.L^{-1}) of the active ingredient	Theoretical content for the active ingredient at 95% (mg) Wi±1.96 $\sigma_{n-1}/\sqrt{n}$	[Flu] mmol.L^{-1} 0 ml / 0 mm / 0 ml / 0 mm	1 ml / 2 mm / 0.025 ml / 0.05	2 ml / 4 mm / 0.05 ml / 0.1 mm	3 ml / 6 mm / 0.15 ml / 0.3 mm	4 ml / 8 mm / 0.25 ml / 0.5 mm	Equation of standard addition at 95% for n-2 $\hat{Y_i} = a \pm s_a t + b \pm s_b t$ [Flu]mmol.L^{-1}	r / r² / R²%
1	Fluconazole Vassil 150 mg Bulgaria	0.2019±0.0230	0.2061	150±17.1173	230	580	891	1200	1552	237.800±36.933+163.200±7.538 [Flu] mmol.L^{-1}	0.9997 0.9994 99.94
					33	78	118	158	208	33.000±7.793+21.500±1.591 [Flu] mmol.L^{-1}	0.9992 0.9984 99.84
					0.240	0.292	0.391	0.814	1.232	0.207±0.051+2.034±0.188[Flu] mmol.L^{-1}	0.9987 0.9975 99.75
2	Candeur Tabuk 150 mg Saudi Arabia	0.2992±0.0071	0.3055	150±3.5811	200	540	845	1125	1392	226.600±65.785+148.450±13.428 [Flu] mmol.L^{-1}	0.9988 0.9976 99.76
					30	75	114	159	194	32.000±7.366+20.600±1.505 [Flu] mmol.L^{-1}	0.9992 0.9984 99.84
					0.235	0.329	0.442	0.934	1.302	0.233±0.064+2.185±0.239 [Flu] mmol.L^{-1}	0.9982 0.9965 99.65
3	Fluconazole Bristol 150 mg UK	0.3573±0.0055	0.3648	150±2.3039	260	610	930	1308	1648	256.400±34.658+173.700±7.074 [Flu] mmol.L^{-1}	0.9998 0.9995 99.95
					34	78	120	168	213	33.000±4.223+22.400±0.862 [Flu] mmol.L^{-1}	0.9998 0.9996 99.96
					0.169	0.348	0.462	0.889	1.298	0.216±0.073+2.196±0.274 [Flu] mmol.L^{-1}	0.9977 0.9954 99.54
4	Diflucan Pfizer 150 mg France	0.3464±0.0041	0.3536	150±1.7823	265	610	998	1289	1688	265.000±65.699+176.250±13.412 [Flu] mmol.L^{-1}	0.9991 0.9983 99.83
					30	69	108	144	190	29.200±6.720+19.750±1.371 [Flu] mmol.L^{-1}	0.9993 0.9986 99.86
					0.183	0.244	0.349	0.684	1.038	0.172±0.022+1.725±0.086 [Flu] mmol.L^{-1}	0.9996 0.9992 99.92

Types of method [Flu] + PTA — Developed method using NAG - 4SX3 - 3D(mV); Classical turbidity; UV- Spectrophotometer at λ $_{max}$= 260nm.

Table 8b: Summary of data for practical content, efficiency (Rec %) for determination of Fluconazole in four samples of drugs and individual t- test for comparison between the means of weight with quoted value, for fluconazole-phosphotungestic acid system

No. of sample	Developed method using NAG - 4SX3 - 3D Analyzer / Classical turbidity / UV- Spectrophotometer at λ_{max}= 260nm. Practical concentration (mmol.L^{-1}) in 10 ml / Practical concentration (mmol.L^{-1}) in 50 ml / Practical weight of Flu. in (g)	Weight of Flu in each sample (g) $\bar{W}_{i(g)} \pm 4.303 \sigma_{n-1}/\sqrt{n}$ / Weight of Flu in tablet $\bar{W}_{i(mg)} \pm 4.303\sigma_{n-1}/\sqrt{n}$	Efficiency of determination Rec.%	Individual t-test between claimed value & practical value ($\bar{W}_{i(mg)}-\mu$) $\sqrt{n}/\sigma_{n-1}$	Paired t –test Compared between three methods $t_{cal}=$ $\overline{w}d \sqrt{n}/\sigma^*_{n-1}$	t_{tab} at 95%confidence level (n-1)
1	1.457 / 9.7141 / 0.1488	0.145689±0.0023	97.126	/-7.9786/ <4.303	Newly developed methodology + quoted value (reference method) -------------------------------- $\bar{X}$d = 0.9303 σ^*_{n-1} = 3.0494 0.6101<<4.303	
1	1.457 / 9.7141 / 0.1488	145.689±2.325	97.126	/-7.9786/ <4.303		
1	1.535 / 10.233 / 0.1567	0.1535±0.0027	102.31	/-7.9786/ <4.303		
1	1.535 / 10.233 / 0.1567	153.465±2.732	102.31	/-7.9786/ <4.303		
1	0.1020 / 10.1990 / 0.1562	0.15295±0.0020	101.97	/-7.9786/ <4.303		
1	0.1020 / 10.1990 / 0.1562	152.955±1.982	101.97	/-7.9786/ <4.303		
2	1.5264 / 10.176 / 0.15583	0.15262±0.0014	101.74	8.1576>4.303		
2	1.5264 / 10.176 / 0.15583	152.620±1.382	101.74	8.1576>4.303		
2	1.5534 / 10.3559 / 0.1586	0.1552±0.0031	103.47	8.1576>4.303	Newly developed methodology and UV- spectrophotometric (classical method) -------------------------------- ---- $\bar{X}$d = -3.4113 σ^*_{n-1} = 4.5516 /-1.4989/ <4.303	
2	1.5534 / 10.3559 / 0.1586	155.212±3.124	103.47	8.1576>4.303		
2	0.1067 / 10.6710 / 0.1634	0.160042±0.0040	106.69	8.1576>4.303		
2	0.1067 / 10.6710 / 0.1634	160.042±3.982	106.69	8.1576>4.303		
3	1.4761 / 9.8407 / 0.15069	0.14759±0.0013	98.39	/-7.8065/ << 4.303		
3	1.4761 / 9.8407 / 0.15069	147.598±1.324	98.39	/-7.8065/ << 4.303		
3	1.4732 / 9.8214 / 0.1504	0.14731±0.0023	98.206	/-7.8065/ << 4.303	Newly developed methodology and turbidity (classical method) -------------------------------- ---- $\bar{X}$d = -1.8928 σ^*_{n-1} = 4.4431 /-0.8520/ <<4.303	
3	1.4732 / 9.8214 / 0.1504	147.308±2.321	98.206	/-7.8065/ << 4.303		
3	0.0983 / 9.8306 / 0.1505	0.14745±0.0028	98.297	/-7.8065/ << 4.303		
3	0.0983 / 9.8306 / 0.1505	147.446±2.832	98.297	/-7.8065/ << 4.303		
4	1.5035 / 10.0236 / 0.15349	0.1503715±0.0020	100.25	0.8076<< 4.303		
4	1.5035 / 10.0236 / 0.15349	150.372±1.982	100.25	0.8076<< 4.303		
4	1.4785 / 9.8565 / 0.15094	0.147865±0.0031	98.57	0.8076<< 4.303		
4	1.4785 / 9.8565 / 0.15094	147.865±3.132	98.57	0.8076<< 4.303		
4	0.0996 / 9.9643 / 0.1526	0.14948±0.0020	99.65	0.8076<< 4.303		
4	0.0996 / 9.9643 / 0.1526	149.481±1.987	99.65	0.8076<< 4.303		

Figure 12: Set of results for comparison between practically content and claimed valve (Individual t-test) and comparison between four methods (Newly developed methodology, turbidity, and the UV-spectrophotometric reference method) using Paired t-test, $\overline{W}$d: average of different between four methods (developed Newly methodology & classical methods), Wd: different between two methods, σ_{n-1}: standard deviation of difference (paired t-test)
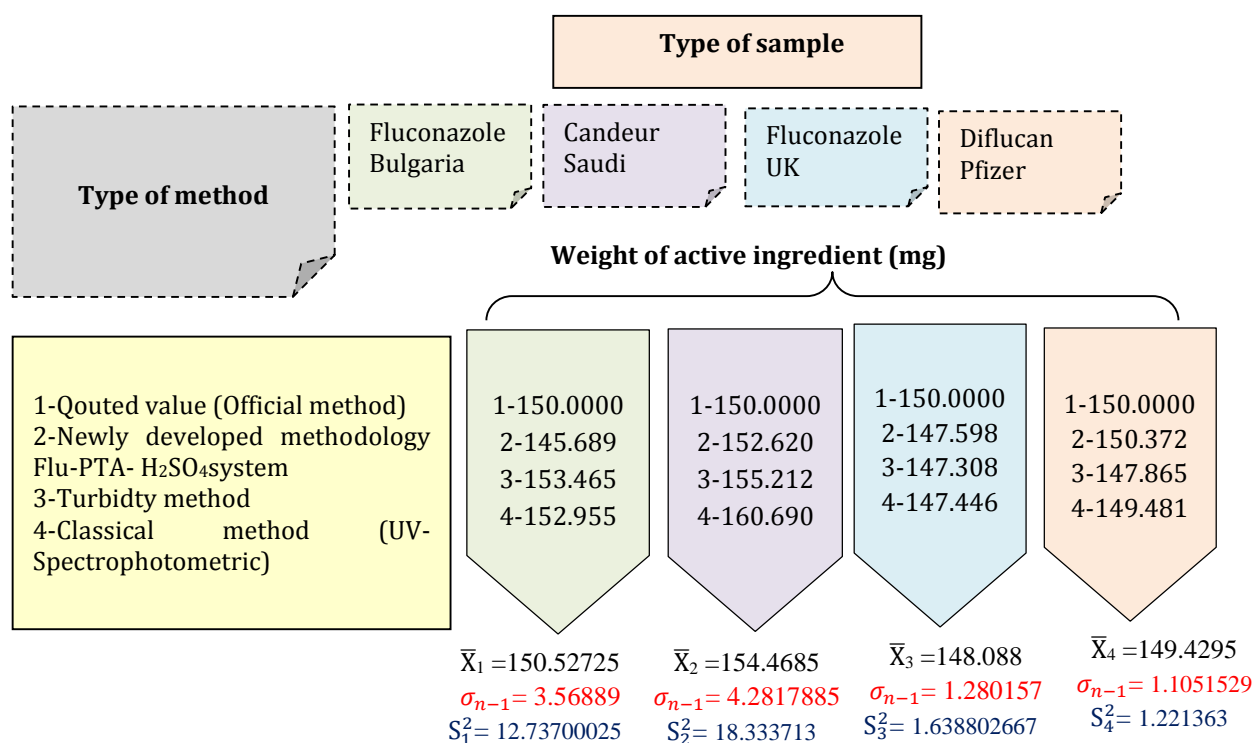
Figure 13: Summed up the results for three different in addition to quoted value and four different samples for

Table 9: ANOVA results for comparison between four different samples from four different Companies

Source	Sum of squares (SSq)	Df	Mean square (MSq)	F_{cal}	$F_{critical}$
Between group	SS_B= 90.59037	3	MS_B=30.19679	3.559801> 3.490295	
Within groups	SS_W=101.7926	12	MS_W=8.48272		
Total	192.383	15			

df = degree of freedom, F_{tab}= $F_{0.95,V1,V2}$= $F_{0.95,3,12}$ = 3.490 at 95% confidence level, K= number of group =4, N=number of measurements or sum of the samples for the groups (i.e) =n_1+n_2+......+n_i =16, SS_B = Sum of squares between group, SS_W = Sum of squares within group, MS_B = SS_B/ K-1 & MS_W = SS_W/ N-K, F_{cal} = MS_B / MS_W.

Conclusion

To investigate fluconazole in pure and pharmaceutical formulations, the recommended Turbidimetric flow-injection method is simple, quick, inexpensive, and sensitive. Fluconazole is precipitated with phosphotungestic acid in an acidic medium, yielding a white ion pair product. The precipitate is calculated by employing a linear array of 12 super white light emitting diodes as a source and three solar cells as a detector to measure the attenuation of incoming light at 0-180°. Compared with spectrophotometry and turbidimetric procedures that employ various precipitating agents, the proposed method uses less expensive apparatus and reagents. The percent R.S.D. was less than 0.5 percent, and all samples were in a good agreement, indicating that the proposed approach is accurate enough. To avoid matrix effects, the conventional additions method was utilized.

Authors' contributions

All authors contributed to data analysis, drafting, and revising of the paper and agreed to be responsible for all the aspects of this work.

ORCID:

Sarah Faris Hameed
https://www.orcid.org/0000-0002-7607-3498

References

[1]. Dayo Owoyemi B.C., da Silva C.C., Souza M.S., Diniz L.F., Ellena J., Carneiro R.L., Fluconazole: synthesis and structural characterization of four new pharmaceutical cocrystal forms, *Crystal Growth & Design*, 2019, **19**:648 [Crossref], [Google Scholar], [Publisher]

[2]. Rewak-Soroczynska J., Sobierajska P., Targonska S., Piecuch A., Grosman L., Rachuna J., Wasik S., Arabski M., Ogorek R., Wiglusz R.J., New approach to antifungal activity of fluconazole incorporated into the porous 6-Anhydro-α-L-Galacto-β-D-Galactan structures modified with nanohydroxyapatite for chronic-wound treatments—in vitro evaluation, *International Journal of Molecular Sciences*, 2021, **22**:3112 [Crossref], [Google Scholar], [Publisher]

[3]. Su S., Shi X., Xu W., Li Y., Chen X., Jia S., Sun S., Antifungal activity and potential mechanism of panobinostat in combination with fluconazole against Candida albicans, *Frontiers in Microbiology*, 2020, **11**:1584 [Crossref], [Google Scholar], [Publisher]

[4]. Vena A., Muñoz P., Mateos M., Guinea J., Galar A., Pea F., Alvarez-Uria A., Escribano P., Bouza E., Therapeutic drug monitoring of antifungal drugs: another tool to improve patient outcome?, *Infectious Diseases and Therapy*, 2020, **9**:137 [Crossref], [Google Scholar], [Publisher]

[5]. Pappas P.G., Kauffman C.A., Andes D.R., Clancy C.J., Marr K.A., Ostrosky-Zeichner L., Reboli A.C., Schuster M.G., Vazquez J.A., Walsh T.J., Zaoutis T.E., Sobel J.D., Clinical practice guideline for the

management of candidiasis: 2016 update by the Infectious Diseases Society of America, *Clinical Infectious Diseases*, 2016, **62**:e1 [Crossref], [Google Scholar], [Publisher]

[6]. Hattab S., Dagher A.M., Wheeler R.T., Pseudomonas synergizes with fluconazole against Candida during treatment of polymicrobial infection, *Infection and Immunity*, 2022, **90**:e00626 [Crossref], [Google Scholar], [Publisher]

[7]. Eşkut N., Gedizlioğlu M., Ünal O., Özlü C., Ergene U., Acute fluconazole toxicity: a case presenting with protean manifestations including systemic and neurologic symptoms, *Postgraduate Medicine*, 2021, **133**:250 [Crossref], [Google Scholar], [Publisher]

[8]. Yang Q., Song K., Hao X., Wen Z., Tan Y., Li W., Investigation of spatial and temporal variability of river ice phenology and thickness across Songhua River Basin, northeast China. *The Cryosphere*, 2020, **14**:3581 [Crossref], [Google Scholar], [Publisher]

[9]. Brewer A.C., Huber J.T., Girardo M.E., Kosiorek H.E., Burns M.W., Stewart T.D., Blair J.E., Cutaneous effects associated with fluconazole in patients treated for coccidioidomycosis, *International Journal of Dermatology*, 2019, **58**:250 [Crossref], [Google Scholar], [Publisher]

[10]. N. Kaur, N. Agnihotri, R. Agnihotri, R.K. Sharma, A Treatise on Spectrophotometric Determination Techniques of Palladium (II) Ions**,** *Journal of* Chemical *Reviews,* 2022, **4**:81 [Crossref], [Google Scholar], [Publisher]

[11]. Padhi R.K., Improvement of Fluidization Quality Using Promoter and Modified Design of Distributor–A Review, *Journal of* Chemical *Reviews,* 2021, **3**:290 [Crossref], [Google Scholar], [Publisher]

[12]. Thakur B., Kumar I., New developed and validated spectroscopic method for the simultaneous estimation of terbinafine hydrochloride and fluconazole, *International Journal of Pharmacy and Pharmaceutical Sciences*, 2020, **12**:19 [Crossref], [Google Scholar], [Publisher]

[13]. Paul S., Mohanram K., Kannan I., Antifungal activity, gas chromatographic-mass spectrometric analysis and in silico study of Punica Granatum

peel extracts against fluconazole resistant strains of Candida species, *Current Pharmaceutical Biotechnology*, 2018, **19**:250 [Crossref], [Google Scholar], [Publisher]

[14]. Virgilio A., Silva A.B.S., Nogueira A.R.A., Nóbrega J.A., Donati G.L., Calculating limits of detection and defining working ranges for multi-signal calibration methods, *Journal of Analytical Atomic Spectrometry*, 2020, **35***:*1614 [Crossref], [Google Scholar], [Publisher]

[15]. Ahmed W., Bivins A., Metcalfe S., Smith W.J., Verbyla M.E., Symonds E.M., Simpson S.L., Evaluation of process limit of detection and quantification variation of SARS-CoV-2 RT-qPCR and RT-dPCR assays for wastewater surveillance, *Water Research*, 2022, **213**:118132 [Crossref], [Google Scholar], [Publisher]

[16]. Holstein C.A., Griffin M., Hong J., Sampson P.D., Statistical method for determining and comparing limits of detection of bioassays, *Analytical chemistry*, 2015, **87**:9795 [Crossref], [Google Scholar], [Publisher]

[17]. Li C., Ashlock J.C., Wang X., Quantifying repeatability reproducibility sources of error and capacity of a measurement: demonstrated using laboratory soil plasticity tests, *Advances in Civil Engineering*, 2019, **2019**:4539549 [Crossref], [Google Scholar], [Publisher]

[18]. Kallner A., Theodorsson E., Repeatability imprecision from analysis of duplicates of patient samples and control materials, *Scandinavian Journal of Clinical and Laboratory Investigation*, 2020, **80**:210 [Crossref], [Google Scholar], [Publisher]

[19]. Bunting K.V., Steeds R.P., Slater L.T., Rogers J.K., Gkoutos G.V., Kotecha D., A practical guide to assess the reproducibility of echocardiographic measurements, *Journal of the American Society of Echocardiography*, 2019, **32**:1505 [Crossref], [Google Scholar], [Publisher]

[20]. Kim T.K., Understanding one-way ANOVA using conceptual figures, *Korean journal of anesthesiology*, 2017, **70**:22 [Crossref], [Google Scholar], [Publisher]

[21]. Liu Q., Wang L., t-Test and ANOVA for data with ceiling and/or floor effects, *Behavior Research Methods*, 2020, **53**:264 [Crossref], [Google Scholar], [Publisher]

Turkie N.S., et al. / Chem. Methodol., 2022, 6(10) 731-749